

First-passage Fingerprints of Water Diffusion near Glutamine Surfaces

Roman Belousov¹, Muhammad Nawaz Qaisrani^{1,2}, Ali Hassanali^{1*}, and Édgar Roldán^{1*}

The extent to which biological interfaces affect the dynamics of water plays a key role in the exchange of matter and chemical interactions that are essential for life. The density and the mobility of water molecules depend on their proximity to biological interfaces and can play an important role in processes such as protein folding and aggregation. In this work, we study the dynamics of water near glutamine surfaces—a system of interest in studies of neurodegenerative diseases. Combining molecular-dynamics simulations and stochastic modelling, we study how the mean first-passage time and related statistics of water molecules escaping subnanometer-sized regions vary from the interface to the bulk. Our analysis reveals a dynamical complexity that reflects underlying chemical and geometrical properties of the glutamine surfaces. From the first-passage time statistics of water molecules, we infer their space-dependent diffusion coefficient in directions normal to the surfaces. Interestingly, our results suggest that the mobility of water varies over a longer length scale than the chemical potential associated with the water-protein interactions. The synergy of molecular dynamics and first-passage techniques opens the possibility for extracting space-dependent diffusion coefficients in more complex, inhomogeneous environments that are commonplace in living matter.

1 Introduction

Proteins and DNA molecules execute their functions mostly in aqueous environments and therefore their interaction with water has become a topic of intense study.^{1–9} Numerous experimental and theoretical studies have shown that the dynamics and thermodynamics of water are altered when in contact with biomolecules.^{2–43} Typically, the diffusive dynamics of water molecules near a protein surface slows down by a factor of four to seven relative to the bulk, and also becomes anisotropic.^{10,12,44} The extent of these dynamical perturbations is thought to play an important role in biological processes.^{44–46}

A class of biological systems that has recently caught our attention, and forms the subject of this work, are proteins that have been implicated in numerous neuro-degenerative diseases—namely, glutamine aggregates.⁴⁷ Like the amyloids, glutamine aggregates are stabilized by dense networks of hydrogen bonds and hydrophobic interactions.^{48–50} Besides their role in biological processes, these systems absorb low-energy photons in the ultraviolet range of wavelengths and, thus, may have promising applications in bio-nanophotonics.^{51–55} Because most of the protein aggregates are formed in aqueous solutions, understanding the solvent's role in nucleation processes is paramount. Recent experiments point to the existence of *water pools*, whose prop-

erties depend on their proximity to the protein fibrils.⁵⁶ As the origins of this dependency are still poorly understood, a quantitative description of the mobility of water close to protein surfaces remains a challenging task.^{10,12,57–59}

In this work we study the diffusive dynamics of water in contact with surfaces of glutamine amino acid crystals⁵⁴. Motivated by our recent work, which showed a surface-sensitive decrease of the water mobility near the liquid-crystal interface,⁶⁰ here we quantify both the magnitude and the length scales over which the solvent's diffusivity is altered. Specifically, we perform molecular-dynamics simulations to extract first-passage time statistics of water molecules to escape nano-sized regions near three different glutamine crystal structures. Combining measurements of first-passage times and stochastic modelling, we develop a method to infer the space-dependent transverse (i.e. in the direction normal to the surface) diffusion coefficient of water as a function of the distance to the interface.

Theory of first-passage times^{61,62} for stochastic processes provides a refreshing perspective that has been successful to describe key phenomena in statistical physics^{63–71}, soft-matter biophysics^{72–76}, astrophysics,^{77–79} finance,⁶² and low-temperature electronics.⁸⁰ Simply put, a first-passage time is defined as the time elapsed until a stochastic process first reaches a target state, e.g. the first time when a Brownian particle reaches a spatial region. Examples include: (i) the first-passage time for one-dimensional (1D) Brownian motion to first cross a threshold located at $L > 0$; (ii) the first-passage time for 1D Brownian motion to first escape through any of the two ends of the interval $[-L, L]$; (iii) the first-passage time for three-dimensional (3D) Brownian motion to escape a cubic cage $[-L, L] \times [-L, L] \times [-L, L]$.

The mobility of water molecules near interfaces, both biolog-

¹ ICTP - The Abdus Salam International Centre for Theoretical Physics, Strada Costiera 11, 34151, Trieste, Italy.

² SISSA - International School for Advanced Studies, Via Bonomea 265, 34136 Trieste, Italy.

* Corresponding authors: AH (ahassana@ictp.it), and ER (edgar@ictp.it).

Requests for materials should be addressed to RB (belousov.roman@gmail.com) and MNQ (mqaisran@ictp.it).

ical and inorganic, and its relation to first-passage times, under various thermodynamic conditions has been a subject of recent works.^{59,81–85} Several approaches, that assume an effective stochastic model of diffusion, have been introduced in order to estimate the inhomogeneous diffusion coefficient from molecular-dynamics simulations.^{10,12,57–59} In particular, it was shown that conditional mean square displacements⁵⁸ and first-passage times subject to various boundary conditions^{59,83} provide means to infer the space-dependent diffusion coefficient for effective models described by Smoluchowski diffusion equations. However, it remains yet an open problem to analyse the range of validity of Langevin models, to explain water diffusion near proteins, and to develop robust comparison and inference methods for the space-dependent diffusivities in soft matter at the nanoscale.

Herein we expand the scope of the first-passage time techniques, to study water diffusivity in contact with crystalline glutamine. We focus on first-passage events of water molecules which, initially located in a small spatial window, escape a subnanometer-sized region. A paradigmatic example is the 1D first-passage time $\tau(z)$ for a water molecule initially located within a thin shell $[z - \delta z/2, z + \delta z/2]$ of width $\delta z > 0$ to cross any of two thresholds located at positions $z - L$ and $z + L$, with $L > \delta z$ defined as a half width of the first-passage corridor (see Fig. 1 for an illustration). The statistics of $\tau(z)$ characterises the kinetics of the ensemble of water molecules at position z near a surface of the glutamine crystal, which we use to probe the glutamine-water interaction dynamics. In particular, we focus on the spatial dependency of the mean time $\langle \tau(z) \rangle$ and the passage probabilities to first cross the positive P_+ or the negative P_- threshold. To gain further insights into the three-dimensional (3D) interactions between the liquid and the protein surface, we extend our approach by considering first-passage times of water molecules escaping from a three-dimensional cubic cage.

Our results show that suitable first-passage statistics reveals "fingerprints" of the underlying diffusive dynamics and the interactions of water molecules with glutamine crystals. Interestingly, parallel to the interface mean first-passage times exhibit a periodic pattern that reflects the underlying chemical and geometrical roughness of the protein surface. Furthermore, the potential arising due to the liquid-crystal interactions induces anisotropies and asymmetries of the first-passage probabilities, which expose preferred directions of the motion of water. Using Langevin dynamics simulations we also investigate the accuracy of the one-dimensional Smoluchowski equation to account for the inhomogeneous diffusion of water in the direction normal to the three surfaces of the glutamine crystal. We demonstrate that this model reproduces statistics of the first-passage events in the water liquid phase above the Gibbs dividing interface. We use these results to develop an inference method for the space-dependent diffusion coefficient of water in the direction normal to the surface by fitting molecular-dynamics mean first-passage times to analytical results derived for the stochastic diffusion model.

The rest of the paper is organised as follows: section 2 begins analysing first-passage time fluctuations in bulk water at atomistic scales. Section 3 discusses first-passage statistics of water molecules escaping 3D regions close to the glutamine crystal—a

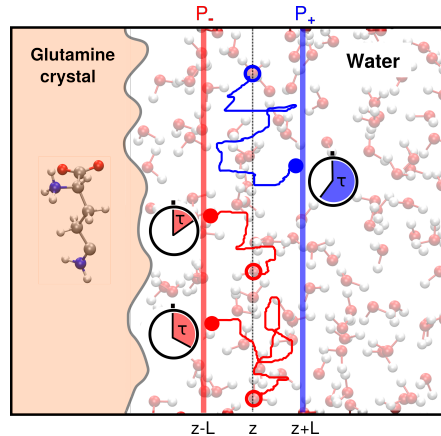


Fig. 1 Sketch of nanoscale measurements of the water molecules' first-passage times in one dimension. Near a glutamine crystal (orange shaded area) water oxygen atoms (open circles) are grouped by their initial positions $z \pm \delta z/2$ into slices of width $\delta z > 0$ along the Z axis, which is perpendicular to the interface plane. Molecules in each group diffuse until they reach boundaries of the corridor $[z - L, z + L]$ at different locations (filled circles) and at a different first-passage time τ (clocks). We measure the times $\tau(z)$ and the probabilities $P_+(z)$ (blue) and $P_-(z)$ (red) that the oxygen atoms reach the absorbing boundary at $z + L$ (blue) or at $z - L$ (red), respectively.

method to probe fine-scale details of surface heterogeneity. Section 4 describes a method to infer space-dependent diffusion coefficient of water near glutamine surfaces, which is applied to the dynamics in the directions perpendicular to three representative protein structures. In Section 5 we analyse the range of validity of state-dependent Markovian diffusion models used in this paper to describe the first-passage time fluctuations of water molecules. We close the paper with a discussion and conclusions in Section 6.

2 Benchmark: bulk water

As a benchmark for our approach we first analyse the diffusive dynamics of bulk liquid water. For this purpose, we use the open-source package GROMACS⁸⁶ to run molecular-dynamics simulations of TIP4P/EW, an empirical potential for water, at density 1 g/cm^3 and at 300 K (see Appendix A for computational details). From the molecular dynamics simulations of bulk water, we extract trajectories containing snapshots of the positions of all the water molecules as a function of time, and then analyse these trajectories as described below.

For the trajectories extracted from molecular dynamics, we evaluate three 1D first-passage times $\tau_X(x)$, $\tau_Y(y)$, and $\tau_Z(z)$ when the oxygen atom of each water molecule travels a distance L from its initial position $q = x, y$, or z along each Cartesian axis X , Y , and Z , respectively. Mathematically, the three first-passage times are defined as follows: $\tau_X(x) = \inf\{t > 0; |X(t) - x| \geq L\}$, $\tau_Y(y) = \inf\{t > 0; |Y(t) - y| \geq L\}$ and $\tau_Z(z) = \inf\{t > 0; |Z(t) - z| \geq L\}$, with $x = X(0)$, $y = Y(0)$ and $z = Z(0)$ the initial values of the (X, Y, Z) coordinates of the trajectories (see Fig. 1 for an illustration of the first-passage time problem along Z). We then combine measurements of $\tau_X(x)$, $\tau_Y(y)$ and $\tau_Z(z)$ in a large sample of a single random variable τ and compute its average $\langle \tau \rangle$, i.e. the global 1D *mean first-passage time*, for different values

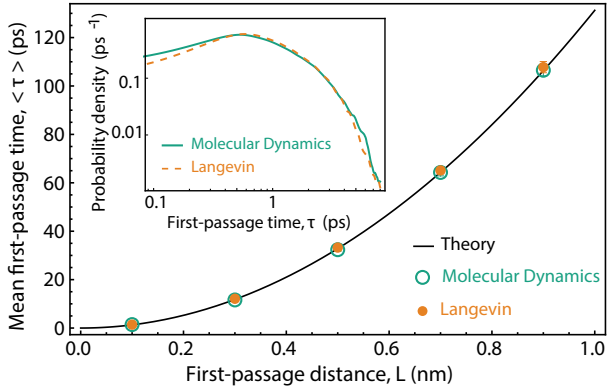


Fig. 2 Mean first-passage time $\langle \tau \rangle$ of oxygen atoms in molecules of bulk water obtained from molecular dynamics (green open circles) and from Langevin simulations (orange filled circles) as a function of the passage distance L . Statistical averages were taken over fixed-size samples of 12411 events. Error bars of the data are smaller than the symbol sizes. Fitting the data points of the molecular-dynamics simulation to a theoretical expression Eq. (1) (black curve) yields an estimate of the bulk water self-diffusion coefficient $D_{\text{bulk}} = (3.81 \pm 0.02) \text{ nm}^2/\text{ns}$. Inset: Probability density of the first-passage time distributions in the molecular dynamics (green solid line) and in the Langevin dynamics (orange dashed line) simulations for $L = 1 \text{ \AA}$.

of L . The mean first-passage time depends on L quadratically $\langle \tau \rangle \sim L^2$ for values of L ranging from 1 \AA to 1 nm . The same scaling law is found for the mean first-passage time of 1D Brownian motion. In a 1D Brownian motion the probability density $P(q, t) \equiv P(q, t | q_0, 0)$ for a coordinate q of a molecule moving with diffusion coefficient D_{bulk} evolves according to a Fokker-Planck equation $\partial_t P(q, t) = D_{\text{bulk}} \partial_q^2 P(q, t)$. In this case a probability distribution of the mean first-passage time (i.e. time elapsed) for a molecule to escape the interval $[q_0 - L, q_0 + L]$ is known and its mean value reads⁶¹

$$\langle \tau \rangle = \frac{L^2}{2D_{\text{bulk}}}. \quad (1)$$

Fitting our measurements to Eq. (1), we estimate the diffusion coefficient of bulk water $D_{\text{bulk}} = (3.81 \pm 0.02) \text{ nm}^2/\text{ns}$, which is consistent with the value determined previously from measurements of mean squared displacements.⁶⁰

We further examine how accurately the overdamped Langevin dynamics describes the first-passage time distributions in bulk water using stochastic simulations. To this end we integrated numerically the stochastic differential equation $dq/dt = \sqrt{2D_{\text{bulk}}}\xi$, in which $\xi(t)$ is Gaussian white noise with the zero mean $\langle \xi(t) \rangle = 0$ and the autocorrelation function $\langle \xi(t)\xi(t') \rangle = \delta(t - t')$. In our Langevin dynamics simulations, we set $D_{\text{bulk}} = 3.81 \text{ nm}^2/\text{ns}$ and use a simulation time step $\Delta t = 1 \text{ fs}$ to harvest a sample of statistically independent first-passage events of the same size and for the same values of L as in our molecular-dynamics simulations. The mean first-passage times $\langle \tau \rangle$ that we obtain from the Langevin dynamics simulations are in excellent agreement with our results from molecular dynamics, for all the range of L that we explore ranging from 0.1 to 1 nm (see Fig. 2). Moreover, even for a distance L as small as 1 \AA , the probability distributions of τ obtained from the molecular-dynamics simulations and Langevin simula-

tions are in excellent agreement (see Fig. 2 inset). This result lends further credence to the one-dimensional model of diffusion and its ability to describe the first-passage time statistics down to atomic-sized corridors of the order of angstroms.

3 3D first-passage statistics of water molecules near glutamine surfaces

Having studied the first-passage time dynamics in the bulk, we move on to discussing the dynamics of water near glutamine. In particular, we analyse in this section first-passage times of water molecules, which escape three-dimensional regions near surfaces of crystalline glutamine. To this aim, we performed three equilibrium molecular-dynamics simulations where a slab of crystalline glutamine (S1, S2, and S3, see left column of Fig. 3) was exposed to approximately 7000 water molecules. As a reference, we orient the Z axis *perpendicular* to the crystallographic planes of these surfaces (see Fig. 3 left column). The molecular-dynamics simulations of the water-glutamine interfaces, which were previously reported by some of us, revealed structural and orientational correlations of the liquid within a shell of 1 nm from the crystal surface.⁶⁰ In order to characterise both the structure and the dynamics of this shell, we determined the Gibbs dividing interface—a plane parallel to the surface of the solid at a position z_{GDI} , at which the water density is half that of the bulk. For more details on the simulation protocol, see Ref.⁶⁰ and Appendix A.

Using the molecular-dynamics trajectories, we analyse structural and dynamical features of a water shell of $1\text{-}\text{\AA}$ thickness projected onto the Gibbs dividing interface (GDI), namely: (i) two-dimensional densities of water molecules $P(x, y)$ (Fig. 3, centre column); and (ii) mean first-passage times $\langle \tau(x, y) \rangle$ (Fig. 3, right column) for the water molecules to escape a cube of edge length $L = 1 \text{ \AA}$ centred at (x, y, z_{GDI}) . Our simulations reveal a clear periodic pattern—at angstrom scales—of the local density of water and their mean first-passage times (Fig. 3). This is consistent with the presence of different chemical groups on the glutamine surface, which make some regions of the surface more accessible than others. In particular, hydrophilic regions, such as the N- and C-termini and the glutamine side chains, lead to enhanced local density and increased first-passage times of nearby water molecules. This is highlighted across the different plots by a green coloured box allowing the reader to see the relationship between the chemical groups, the water density and the first passage times.

The coupling between the water density and first-passage times, while interesting, is not so surprising. More intriguing is perhaps the extent to which the fingerprints of the structure and dynamics can still be observed, as the projecting plane of the middle and right columns in Fig. 3 moves further away from the crystal surface. At longer distances from the crystal, on the order of a few angstroms from the Gibbs dividing interface, the periodic pattern of $P(x, y)$ and $\langle \tau(x, y) \rangle$ fades gradually (Fig. 4). In particular, beyond 5 \AA we do not observe any of the patterns in the 2D densities and the mean first-passage times observed in Fig. 3.

In order to establish a measure on the range at which the 3D passage statistics provide a fingerprint of the interaction between

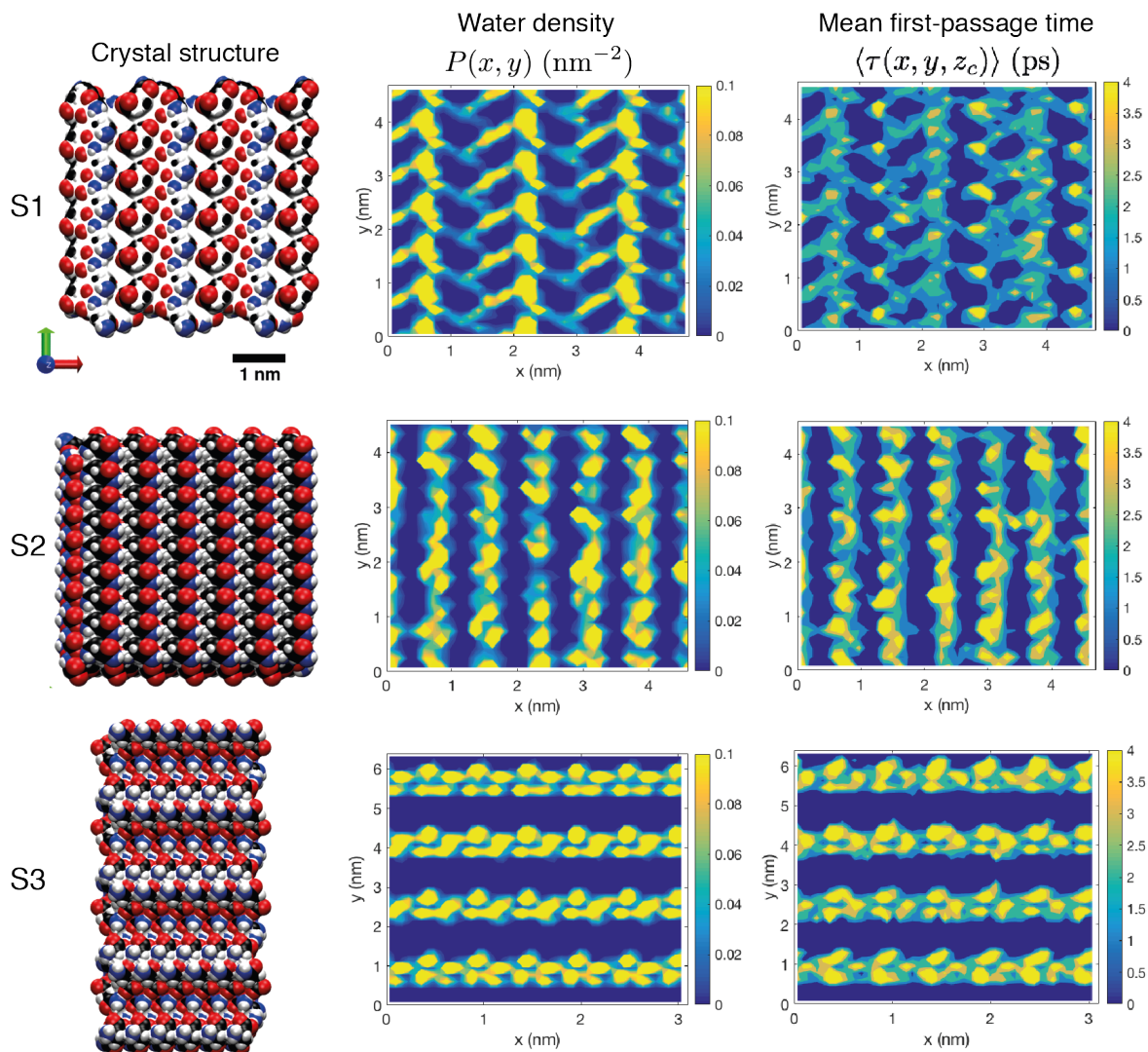


Fig. 3 First-passage time fingerprints in water molecules diffusing near glutamine crystals. Three surfaces of the glutamine crystal slab: crystal structures of the respective crystallographic planes perpendicular to the Z axis (left column), density histograms $P(x, y)$ of water molecules (centre column) and their mean first-passage times $\langle \tau(x, y) \rangle$ to escape a cube of edge length $L = 1 \text{ \AA}$ (right column). In the crystal structures, we show hydrogen atoms in white, oxygen in red, nitrogen in blue, and carbon in black. The 2D plots represent 3D data that were collected in a shell of thickness 1 \AA and projected onto the median XY plane centred at the Gibbs dividing interface.

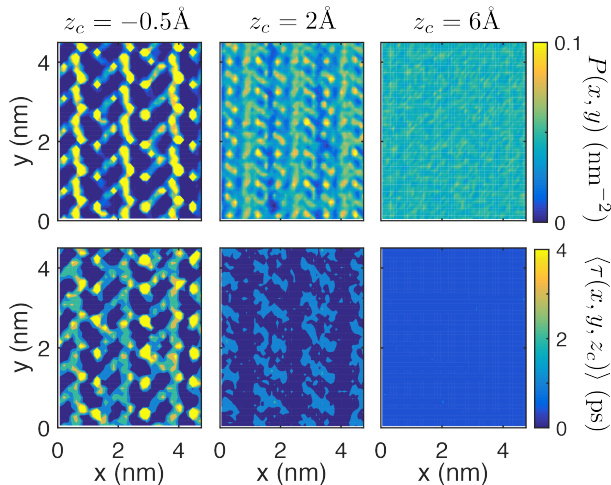


Fig. 4 Local density $P(x,y)$ (top row) and mean first-passage times $\langle \tau(x,y,z_c) \rangle$ of water molecules to escape a cube of edge length 1 \AA centred at (x,y,z_c) (bottom row) for various distances z_c from the glutamine surface S1: 0.5 \AA below (left column), 2 \AA above (middle column), and 6 \AA above (right column) the Gibbs dividing interface.

water and glutamine surface, we examined two first-passage parameters as a function of separation distance between the first-passage cube and the glutamine surfaces: (i) the passage probabilities P_x , P_y and P_z for water molecules to first exit a 1 \AA^3 volume cube through any of its faces perpendicular to the X , Y or Z axes; and (ii) the corresponding *conditional* mean first-passage times $\langle \tau_x \rangle$, $\langle \tau_y \rangle$ and $\langle \tau_z \rangle$ associated with these events. We report in Fig. 5 the value of these parameters as a function of distance from the surfaces S1, S2 and S3.

The structure of the 3D passage probabilities is quite sensitive to the distance from the protein surface: for the three glutamine surfaces, the passage probabilities are asymmetric below the Gibbs dividing interface, and they all saturate to the bulk value of $1/3$ at a distance of $\sim 5 \text{ \AA}$. While for surface S1 all the three components (P_x , P_y and P_z) are quite similar at about 0.2 nm , in the case of S2 and especially S3, the passage probabilities exhibit a rather pronounced symmetry breaking. On the other hand, the conditional mean first-passage times appear to be characterised by a different phenomenology. Below the Gibbs dividing interface, the mean first-passage times are increased up to one order of magnitude with respect to their bulk value consistent with our earlier studies, where we found an increase of the water molecules' residence times near the surface.⁶⁰ Above the interface, our simulations reveal a symmetry $\langle \tau_x \rangle = \langle \tau_y \rangle = \langle \tau_z \rangle$ between the conditional mean first-passage times in different directions. This symmetry extends also to distances below 5 \AA , at which the passage probabilities are *not* symmetric. It is clear that the first-passage statistics lose their x and y dependence as we move further away from the surface and hence this motivated us to study the dynamics of water along Z direction. This forms the subject of the following section.

4 1D first-passage of water near glutamine: method to infer space-dependent diffusivity

In this section we study the dynamics of water molecules projected onto the Z coordinate axis—the direction perpendicular to the surface of contact with the glutamine crystals. Using our molecular-dynamics simulations, we measure the stationary spatial density of water molecules $P(z)$ that varies with the distance z from the Gibbs dividing interface (Fig. 6, first column).⁶⁰ For the three surfaces we find that $P(z)$ increases with the separation distance from the interface, saturating to the bulk value at distances greater than $5\text{--}6 \text{ \AA}$ from the Gibbs dividing interfaces. In the case of S2 and S3, the water density near these glutamine crystals has a pronounced minimum close to the Gibbs dividing interface, and a maximum below it. This result reveals presence of hydrophilic *pockets* coupled with the underlying geometric roughness of the surfaces S2 and S3, which admit a deep penetration of water. For the glutamine crystal S1, we do not observe these phenomena but a smooth increase of the water density as a function of the distance perpendicular to the surface.

To further understand the kinetics of water molecules in the direction perpendicular to the surfaces, we measure the mean first-passage time for water molecules along the Z axis. As we will see below, the mean first-passage time $\langle \tau(z) \rangle \equiv \langle \tau_z(z) \rangle$ with $L = 1 \text{ \AA}$ along the Z axis (Fig. 1) provides insights into the transverse mobility of water molecules that reside at a distance z from the protein surface. Figure 5 (bottom row) shows the values of *conditional* mean first-passage times $\langle \tau_+(z) \rangle$ and $\langle \tau_-(z) \rangle$ for water molecules to first escape the first-passage corridor $[z-L, z+L]$ through its positive or negative end, respectively. In the wetting layer of all the three glutamine surfaces—below the Gibbs dividing interfaces—we observe a strong anisotropy of the conditional mean first-passage times $\langle \tau_+(z) \rangle \neq \langle \tau_-(z) \rangle$. As z grows, the magnitude of these two first-passage times decrease and eventually converge to the bulk value away from the interface, $\langle \tau(z) \rangle = \langle \tau_+(z) \rangle = \langle \tau_-(z) \rangle$ for $z \gg 5 \text{ \AA}$. The decay of the mean first-passage times towards bulk value as a function of distance from the surface, is not monotonous for the surfaces S2 and S3. In particular, we observe a fast dynamics of water molecules with a local minimum of the conditional mean first-passage times in a region of low local density where the chemical potential is large.

Motivated by recent results describing fluctuations of water density at the nanoscale with effective stochastic models,^{12,58,59} we investigate next whether our measurements of molecular density and mean first-passage times can be explained by such a mathematical model. We consider a paradigmatic model of a one-dimensional inhomogeneous diffusion along the Z axis with a space-dependent diffusion coefficient $D(z)$ in presence of a potential $U(z)$. In this model, the evolution of the density of the fluid $P(z,t)$, which depends on the spatial coordinate z and time t , obeys the Smoluchowski equation

$$\frac{\partial P(z,t)}{\partial t} = \frac{\partial}{\partial z} \left(\beta D(z) P(z,t) \frac{\partial U(z)}{\partial z} + D(z) \frac{\partial P(z,t)}{\partial z} \right), \quad (2)$$

where $\beta \equiv (k_B T)^{-1}$, with k_B Boltzmann's constant, T the temperature of the fluid. In Eq. (2) we have assumed Einstein's relation

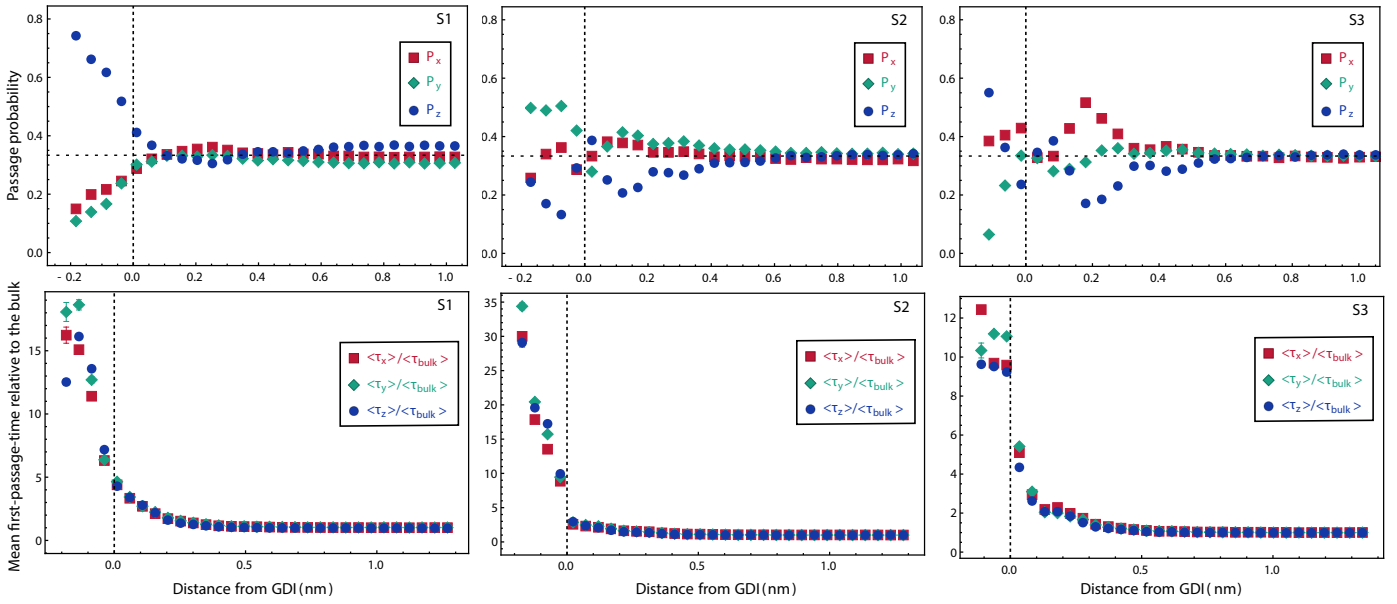


Fig. 5 Top row: passage probabilities $P_X(z)$, $P_Y(z)$ and $P_Z(z)$ for water molecules to escape a cube of side $L = 0.1$ nm through the faces perpendicular to X , Y , and Z axes, respectively, as functions of the distance from the Gibbs dividing interface with the glutamine surfaces S1 (left), S2 (middle) and S3 (right). Bottom row: mean first-passage times $\langle \tau_X(z) \rangle$, $\langle \tau_Y(z) \rangle$, and $\langle \tau_Z(z) \rangle$ conditioned on the escape events through the corresponding sides of the cube and normalised with respect to the bulk-water value $\langle \tau_{\text{bulk}} \rangle = (0.623 \pm 0.007)$ ps. Both the probabilities and the mean first-passage times are obtained by averaging over all events detected in cubes, whose geometric centres are located at (x, y, z_c) with z_c fixed at a given distance from the Gibbs dividing interface.

for the mobility $\mu(z) = \beta D(z)$. The right-hand side of the Smoluchowski equation represents the negative divergence of the drift current $-\mu(z)P(z)U'(z)$ and Fick's diffusion flow $-D(z)P'(z)$.

For the Smoluchowski diffusion model described by Eq. (2) quadrature formulas for mean first-passage times with two absorbing boundaries have been derived (see Appendix C).^{64,87} These formulas are amenable to a complete analytical treatment only for special cases of $U(z)$ and $D(z)$. Here we consider the limit of a small passage corridor width L by taking a linear-order approximation for $U(z)$: $U(z + \varepsilon) \simeq U(z) + U'(z)\varepsilon$ with $\varepsilon \in [z - L, z + L]$. Furthermore, as we show in Appendix D, the diffusion coefficient of water near the three glutamine surfaces S1, S2, and S3 varies much slower with z . As a result, it can be approximated by a constant value over the entire first-passage corridor, i.e. $D(z + \varepsilon) = D(z)$ for $\varepsilon \in [z - L, z + L]$. This approximation is consistent with previous work showing that the effective diffusion coefficient in water-peptide systems varies slower than the relevant interaction potential.⁵⁸ Taking the Smoluchowski model described by Eq. (2) and the aforementioned approximations $U(z + \varepsilon) \simeq U(z) + U'(z)\varepsilon$ and $D(z + \varepsilon) = D(z)$ for any $\varepsilon \in [z - L, z + L]$, we derive the following formula for the mean first-passage time to escape the corridor $[z - L, z + L]$ (see Appendix C)

$$\langle \tau(z) \rangle \simeq \frac{L \tanh(L\beta U'(z)/2)}{D(z)\beta U'(z)}. \quad (3)$$

Note that in the limit of $L\beta U'(z)$ being small, Eq. (3) yields $\langle \tau(z) \rangle \simeq L^2/2D(z)$ and, thus, recovers the quadratic dependency of the mean first-passage time on L obtained in the bulk, given by Eq. (1).

From our measurements of the local stationary density of water molecules $P(z)$ (Fig. 6 left column) and their mean first-passage times $\langle \tau(z) \rangle$ (Fig. 6 right column), we determine the effective water-glutamine chemical potential $U(z)$ and then infer the space-dependent diffusivity $D(z)$ for the three glutamine crystal structures. The inference method proceeds as follows. First, we obtain the effective potential as $\beta U(z) = -\ln P(z)$. Second, plugging this result into Eq. (3) we obtain an estimate for the diffusion coefficient $D(z) \equiv L \tanh(L\beta U'(z)/2)/U'(z)\langle \tau(z) \rangle$ in terms of L , the mean first-passage time $\langle \hat{\tau}(z) \rangle$ and the local density $P(z)$.^{*} In our estimates we used the trajectories from molecular-dynamics simulations previously described in Sec. 2 and a narrow passage corridor of half width $L = 1 \text{ \AA}$.

Figure 7 shows the values of $U(z)$ and $D(z)$, inferred from our molecular-dynamics simulations for water molecules near the three surfaces of the glutamine crystal. Consistent with the water density profiles, the effective potentials associated with the surfaces S2 and S3 are characterised by large energy barriers that separate the protein-wetting layer from the liquid phase above the Gibbs dividing interface. The space-dependent diffusion coefficient also features some oscillations near the surface. Specifically, the peaks in the local diffusion constant close to the interface appear to be located close to the positions of the maxima associated with the underlying potential. More interesting is the difference of the length scales over which the potential and the diffusion coefficient approach their bulk values. For all the three water-

* The spatial derivatives were evaluated numerically, using a pseudospectral approach (see Appendix B).

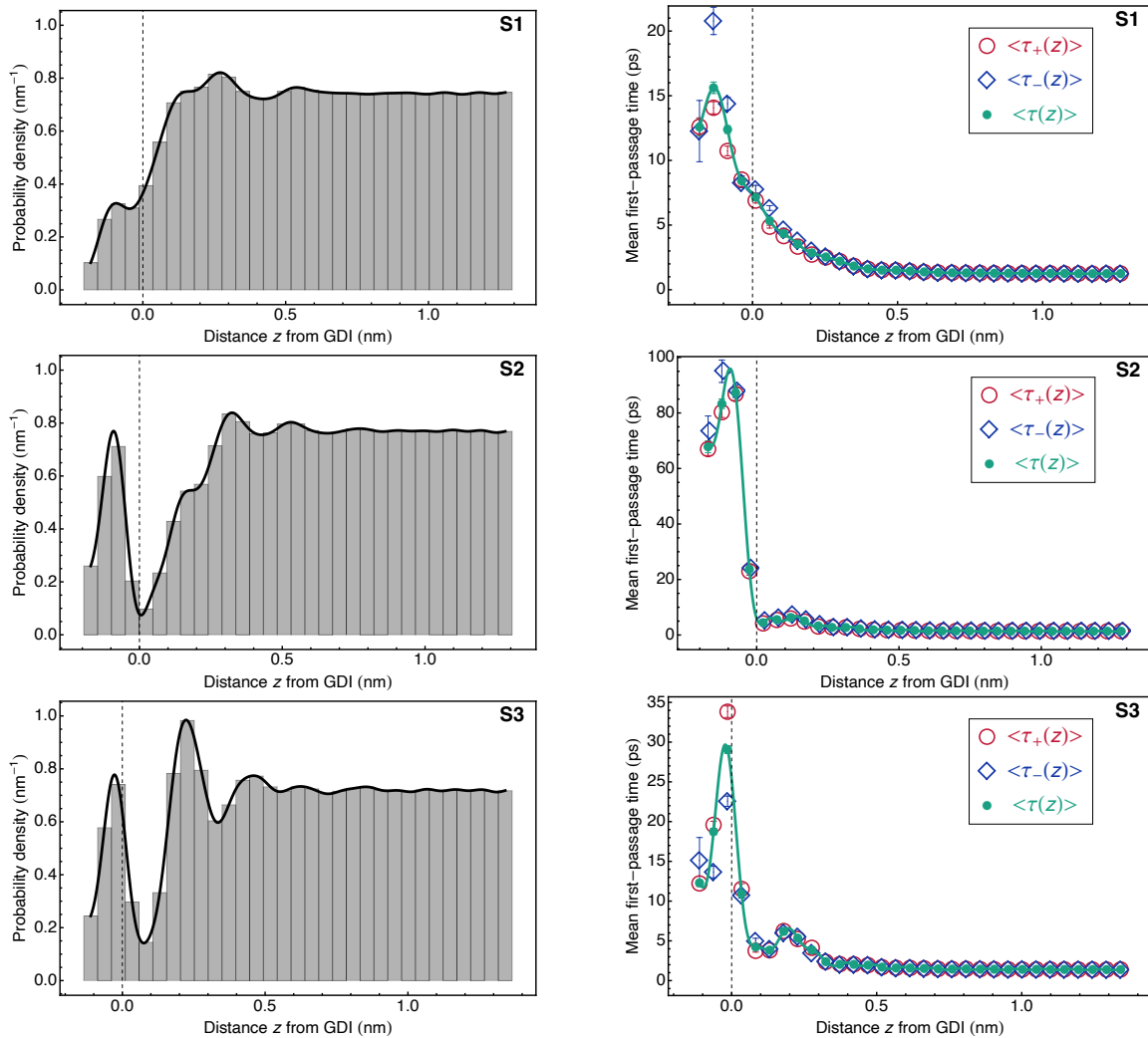


Fig. 6 Density histograms (left panels) and 1D mean first-passage times to escape the interval $[z-L, z+L]$ with $L = 1 \text{ \AA}$ (right panels) for water molecules residing initially at a distance z from the Gibbs dividing interface (GDI) of the glutamine crystals S1, S2 and S3. The vertical dashed lines mark the Gibbs dividing interface ($z=0$), whereas the solid lines represent trigonometric interpolations.

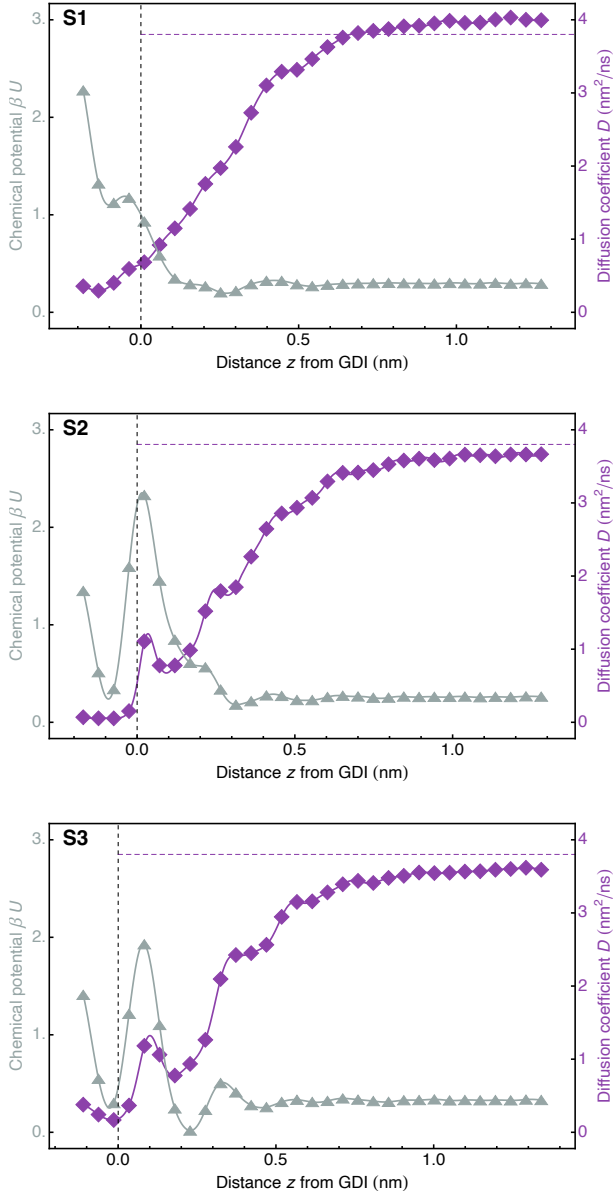


Fig. 7 Inference of space-dependent effective diffusion coefficient and potential from first-passage and density measurements of water molecules near glutamine. Estimates of the space-dependent transverse diffusion coefficient $D(z)$ (purple diamonds, right axis) and the effective chemical potential $U(z)$ (gray triangles, left axis) for water molecules as functions of the distance z to the Gibbs dividing interface of crystalline-glutamine surfaces S1 (top), S2 (middle), and S3 (bottom). Solid lines are trigonometric interpolations of the data. The purple dashed horizontal lines are set at the diffusion constant value of the bulk water $D_{\text{bulk}} = 3.81 \text{ nm}^2/\text{ns}$.

glutamine contacts simulated, the potential $U(z)$ flattens out at distances of about 5 \AA from the respective Gibbs dividing interface. In contrast, the space-dependent diffusivity extends over a longer range: the diffusion coefficient approaches its bulk value at about 10 \AA from the surfaces. For large distances, the relative error of our estimates of $D(z)$ with respect to the bulk value 5–6 %, a result that stems from the uncertainty of the inferred slope of the potential $U'(z)$.

The specific origin of why the diffusion coefficient saturates over a longer length scale in comparison with the range of the associated chemical potential is not so obvious and we cannot pinpoint any particular reasons at this moment. We remark however, that the density $P(z)$ and the mean first-passage time $\langle \tau(z) \rangle$, that are used to reconstruct $U(z)$ and $D(z)$, integrate out other degrees of freedom that may be playing a role in tuning the dynamics. In our previous work, we also examined how the orientational correlations and the charge density of the water molecules change as functions of the distance from the Gibbs dividing interface (see Figure 4 in Ref.⁶⁰). We observed therein subtle spatial patterns of the water charge density, suggesting that the glutamine surface induces perturbations of the electrostatic potential created by the solvent, which are not reflected in the mass density.

5 Exploring the validity of Langevin models

The preceding analysis has revealed a slowdown of the water dynamics due to the strong electrostatic potential arising from the charged chemical groups of the glutamine molecule. A key assumption in our first-passage analysis is that the translational dynamics of water is well described by a Markovian diffusion model, which at the ensemble level, is characterised by the Smoluchowski equation (2). To verify this assumption and to lend more credence to this theoretical approach, we compare in Fig. 8 first-passage time statistics obtained in our water-glutamine molecular dynamics simulations (Sec. 4) with first-passage times obtained from numerical stochastic simulations of space-dependent diffusions. For the latter, we performed *a posteriori* numerical simulations of the overdamped Ito-Langevin equation

$$\frac{dz}{dt} = -\beta D(z)U'(z) + D'(z) + \sqrt{2D(z)} \cdot \xi, \quad (4)$$

where $\xi(t)$ is Gaussian white noise, whereas $U(z)$ and $D(z)$ are, respectively, the effective potential and the space-dependent diffusion coefficient of water inferred from our molecular-dynamics simulations (see Sec. 4 and Appendix B). Note that the so-called spurious drift term $D'(z)$ in Eq. (4) ensures that the Fokker-Planck equation describing ensembles of trajectories generated by (4), coincides with the Smoluchowski equation (2).⁸⁸ In order to examine the sensitivity of our results to the presence of a space dependent diffusion constant, we also perform numerical simulations of an overdamped Langevin equation

$$\frac{dz}{dt} = -\beta D_{\text{bulk}}U'(z) + \sqrt{2D_{\text{bulk}}} \cdot \xi. \quad (5)$$

with $D_{\text{bulk}} = 3.81 \text{ nm}^2/\text{ns}$ bulk water's (space-independent) diffusion coefficient $U(z)$ given by water's effective chemical potential as in Eq. (4).

From numerical simulations of Eqs. (4) and (5), we evaluate mean first-passage times $\langle\tau(z)\rangle$ and passage probabilities $P_+(z)$ and $P_-(z)$ (see Fig. 1) to escape the corridor $[z-L, z+L]$ with $L = 1\text{\AA}$. We compare these statistics in Fig. 8 with the data obtained from our molecular-dynamics simulations reported in Sec. 4. The mean first-passage times of the inhomogeneous Langevin model Eq. (4) are in good agreement with those obtained in the molecular-dynamics simulations, both capturing the slowdown associated with the mobility of water near all the three glutamine surfaces. Above the Gibbs dividing interface, the Langevin model yields slightly larger first-passage times than molecular dynamics in the bulk liquid, as reported previously in Ref.⁵⁹. On the other hand, the homogeneous diffusion model (5) fails completely to capture the complexity as well as the magnitude of the mean first-passage time of water molecules (left column of Fig. 8) at distances $z < 0.5\text{ nm}$ from any of the three glutamine surfaces.

The passage probabilities $P_+(z)$ and $P_-(z)$ (Fig. 8, right column) provide further insights into the behavior of water near the glutamine surface. Interestingly, the passage probabilities obtained from simulations of the Langevin model (4) are in excellent agreement with those obtained from the molecular dynamics, reproducing local maxima and minima above the Gibbs dividing interface for the three glutamine crystals S1, S2 and S3. On the other hand, the Langevin model given by Eq. (4) is not able to capture accurately the non-trivial behaviour of the passage probabilities $P_+(z)$ and $P_-(z)$ for water molecules that are closely pinned to the glutamine surface. This phenomenon is also observed for the mean first-passage time $\langle\tau(z)\rangle$ (Fig. 8, left column).

To obtain a more quantitative perspective of the validity of the Langevin model, we employ some recent results invoking the extent of *first-passage time symmetry* derived within the context of stochastic thermodynamics and random walks.^{89–91} For an homogeneous Langevin equation $dz/dt = v + \sqrt{2D} \cdot \xi$ with v and $D > 0$ as two given parameters, the probability densities of the conditional first-passage times $\tau_+(z)$ and $\tau_-(z)$ are identical.^{89–91} This result implies a symmetry between the conditional mean first-passage times

$$\langle\tau_+(z)\rangle = \langle\tau_-(z)\rangle, \quad (6)$$

which holds for any values of the drift v and diffusion coefficient D . We put Eq. (6) to test using the data from our molecular dynamics simulations. For narrow first-passage corridors, $U(z)$ and $D(z)$ in Section 4, Eq. (4) yields an effective local homogeneous Langevin equation $\frac{dz}{dt} \simeq v(z) + \sqrt{2D(z)} \cdot \xi$ with $v_Z(z) = \beta U'(z)$ and $D(z)$ referring to the local slope of the potential and diffusion coefficient, respectively. Therefore, if our approximations are viable, we expect the symmetry Eq. (6), *i.e.* $\langle\tau_+(z)\rangle = \langle\tau_-(z)\rangle = \langle\tau(z)\rangle$, to hold within narrow passage corridors at any distance from the glutamine surface. To quantify the degree of violation of the first-passage time symmetry (6) we introduce a measure of accuracy

$$\delta_{\pm}(z) = \left(1 - \frac{|\langle\tau_+(z)\rangle - \langle\tau_-(z)\rangle|}{\langle\tau(z)\rangle}\right) \times 100, \quad (7)$$

which characterises the relative difference (in %) between the

two conditional mean first-passage times with respect to the total mean first-passage time along the Z axis. An accuracy $\delta_{\pm}(z) = 100$ implies a perfect agreement, whereas $\delta_{\pm}(z) = 0$ a strong violation of the first-passage symmetry (6).

We report values of $\delta_{\pm}(z)$ given by Eq. (7) in Fig. 9, which shows that the first-passage symmetry holds within an accuracy of at least 75 % at distances $z \gtrsim 1\text{\AA}$ from the Gibbs dividing interfaces of water with all the three glutamine surfaces S1, S2, and S3 (Fig. 9). For water molecules located closer to the glutamine surface, we find statistically significant deviations from the symmetry Eq. (6)—a result that challenges the validity of the Langevin model (4) and the approximations used in our estimates below the protein-wetting layer. In order to verify that this discrepancy is not caused by linear-order effects of the inhomogeneous diffusion, we have estimated the mobility of water molecules by using a more complex diffusion model (Appendix D) and found no appreciable changes in our results (Fig. 10).[†]

In conclusion, the preceding analysis reveals the limits of the ability of the Smoluchowski diffusion model to explain the dynamics of water molecules that remain for a long time closely pinned to the glutamine surface. Earlier, we showed by examining the 3D first-passage statistics that the diffusive dynamics of molecules with the same coordinate z and various coordinates x and y can differ substantially. Hence, the projection of this dynamics on a single coordinate axis may mix populations of water molecules with different dynamical properties. In such a complex environment alternative approaches that take into account inhomogeneous distributions of microscopic displacements and/or nonlocal and memory effects^{9,92–95} may provide further insights into water dynamics below the Gibbs dividing interface.

6 Conclusions

In this work, we have shown that first-passage times of water molecules at atomic scales carry information about their dynamical interaction with glutamine crystals. We have used a combination of atomistic molecular-dynamics simulations and stochastic methods of stochastic theory to characterise the mobility of water molecules near crystalline glutamine. This system is a useful model for understanding how the diffusive dynamics of water is perturbed by protein aggregates, a problem that is highly relevant in studies of neurodegenerative diseases and crystal nucleation.

First-passage statistics of water molecules in the molecular-dynamics simulations were analysed as a function of distance from three crystallographic planes of the glutamine crystal. We showed that the mean time and a plethora of related first-passage statistics provide fresh insights for modelling the diffusive dynamics of water molecules in contact with a crystal surface and more generally biological systems. Interestingly, the passage probabilities of water molecules appear to be more sensitive to anisotropies in different directions as a function of distance from the surface compared to the mean first passage times.

Fitting our data to an inhomogeneous diffusion model, we

[†] We remark that the magnitude of the first-passage corridor L cannot be reduced below 1\AA —the length scale of a covalent bond.

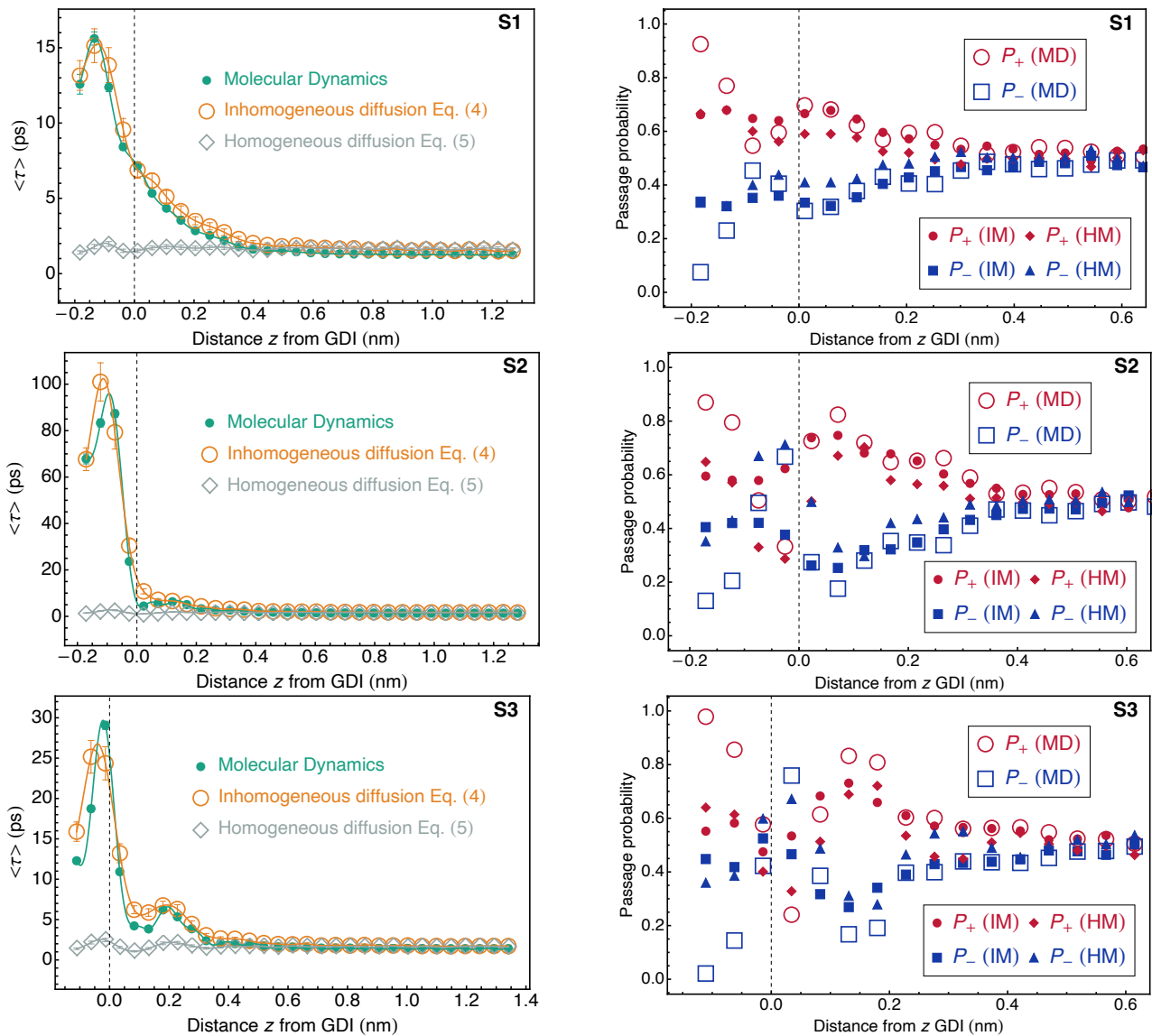


Fig. 8 Comparison between the first-passage statistics obtained in our molecular-dynamics simulations of the water-glutamine contacts S1–3 (MD) with the same statistics measured in numerical simulations of two stochastic equations—the inhomogeneous stochastic diffusion model [IM, Eq. (4)] and the homogeneous stochastic diffusion model [HM, Eq. (5)]. Left panels: mean first-passage time $\langle \tau(z) \rangle$ as a function of the distance from the Gibbs-dividing interface. Right panels: passage probabilities $P_+(z)$ and $P_-(z)$ for water molecules to first reach the positive and negative end of the first-passage corridor $[z - L, z + L]$ ($L = 1 \text{ \AA}$). The solid lines are trigonometric interpolations of the data points. The total number of first-passage events analyzed for each value of z was 10^4 – 10^5 in our molecular-dynamics simulations and 10^3 in our stochastic simulations.

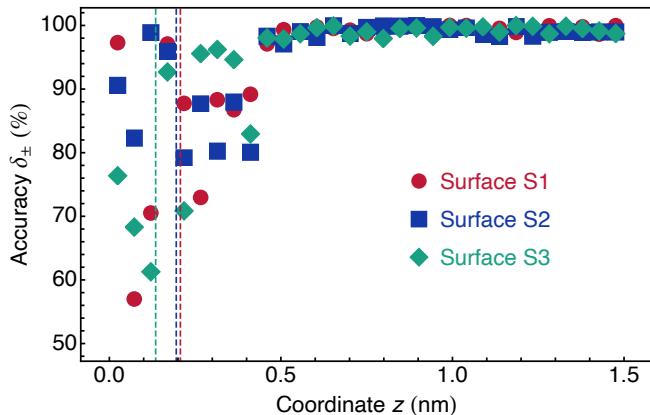


Fig. 9 Accuracy measure $\delta_{\pm}(z)$, given by Eq. (7), of the first-passage time symmetry (6) obtained for our water-glutamine molecular-dynamics simulations as a function of the distance z to the contact with the three glutamine surfaces (see legend). The vertical dashed lines indicate the location of the Gibbs dividing interfaces between the liquid and glutamine crystal.

have reconstructed the transverse space-dependent diffusion coefficient of water molecules as a function of distance to each of the three glutamine surfaces. Our measurements reveal a slow-down of the solvent’s diffusive dynamics near the protein almost by a factor of 4 relative to the bulk. Curiously, the chemical potential of the water molecules does not extend far beyond 0.5 nm from the Gibbs dividing interface, whereas the diffusion constant saturates slowly to the bulk value approximately at 1 nm. This may reflect the longer range of orientational and charge correlations in the water as well as the fact that the diffusion is more sensitive to the excluded volume induced by the presence of the crystal surface.

The combination of both the molecular-dynamics simulations and stochastic modelling provides us with a robust method to estimate space-dependent diffusion coefficients from mean first-passage times to escape narrow corridors, valid not only in atomic but also at mesoscopic scales. This approach can be applied to a plethora of different systems and opens up the possibility for interesting applications including understanding the diffusion tensor of water molecules around more complex and disordered interfaces.^{96–98} Besides this, the first-passage distributions open up some interesting directions on trying to use them to identify chemical fingerprints for hydrophobic and hydrophilic environments. The application of these methods will be the subject of forthcoming studies in our group. This will also help in the interpretation of the experimental measurements of water structure and dynamics near biological surfaces.^{99,100}

Conflicts of interest

There are no conflicts to declare.

Acknowledgements

We thank Francesco Sciortino, Jacopo Grilli, the Grill lab, the Pavin group, the Tolic lab, and Peter Hänggi for stimulating discussions.

Appendix

A Molecular dynamics.

All the molecular dynamics simulations for the three surfaces were performed with the GROMACS package.⁸⁶ In all these simulations, we used the OPLS-AA¹⁰¹ force field together with the TIP4P water model.^{102,103} A non-bonded pair list was created with a cut-off radius of 1.4 nm and updated after every 10 time integration steps. For the shifted Lennard-Jones potential, the cut-off was set at 1.2 nm. The long-range electrostatic forces were taken into account by using the Particle Mesh Ewald-Switch¹⁰⁴ method with a Coulomb switching cut-off 1.2 nm. A long-range dispersion correction for the pressure and energy was applied to the truncated van der Waals interactions. All bonds were constrained using the LINCS algorithm.¹⁰⁵ A timestep of 2fs was used for the Verlet integrator. All simulations were performed in the canonical ensemble (NVT) at 300K using the velocity-rescale thermostat¹⁰⁶ with a time-constant of 0.1 ps.

B Data analysis.

Statistical data were collected from 15-ns-long trajectories for each of the three water-glutamine interfaces, and from a 2-ns-long trajectory for the bulk water. Positions of water molecules were identified with the coordinates of the oxygen atoms in the H₂O groups.

The effective potential $U(z)$ associated with the glutamine surfaces was extracted from histograms of the water density (Sec. 4). We inspected an interval of length $\ell = 1.5$ nm along the Z coordinate axis in the immediate contact with the glutamine crystal. This interval was partitioned into $\nu = 31$ bins of equal size. Values of the histogram density were assigned to the bins’ centres $z_{i=1,2,\dots}$, which thus form an equidistant grid of points. In addition we assume zero-gradient boundary conditions: thermodynamic properties have no spatial variation for large z in contact with the bulk liquid, whereas at the protein end of the inspected interval we impose a fictitious reflective boundary condition.

A pseudospectral basis set,¹⁰⁷ that is appropriate for the above boundary conditions and nodes, is given by trigonometric functions

$$\phi_n(z) = \begin{cases} \sqrt{2/\ell} & \text{if } n = 0, \\ \cos(\pi n z / \ell) / \sqrt{\ell} & \text{if } 0 < n < 30, \end{cases} \quad (8)$$

which are orthonormal with respect to the weight $\delta z = \ell / \nu \approx 0.03$ nm and the scalar product

$$\langle \phi_n(z), \phi_m(z) \rangle = \delta z \sum_{i=0}^{\nu-1} \phi_n(z_i) \phi_m(z_i).$$

Any function $f(z)$ that satisfies the same boundary conditions, such as $U(z)$ and $\ln D(z)$, can therefore be represented by

$$f(z) = \sum_{n=0}^{\nu-1} f_n \phi_n(z), \quad f_n = \langle \phi_n(z) | f(z) \rangle. \quad (9)$$

This trigonometric interpolation ensures spectral accuracy of numerical calculations with empirical functions.¹⁰⁷ We have verified that the pseudospectral representation of the steady-state density

with the chosen number of the bins ν renders a density estimate that is as efficient as a smooth histogram with the Epanechnikov kernel.

The first-passage events were detected with a time resolution of $\delta t = 50$ fs for molecules' displacements of length $L = 1$ Å in any direction from the initial positions $z(0) = z$. To mitigate the discretization effect of the data acquisition we subtracted from each time measurement t of the first-passage event a linear-order correction

$$\tau(z) = t - \delta t \frac{L - |z(t - \delta t) - z|}{|z(t) - z(t - \delta t)|}.$$

We have also checked that our choice of δt does not have a strong influence on the results, by using a higher resolution $\delta t = 6$ fs with trajectories of a shorter duration (5 ns).

The first-passage times were averaged over the water molecules residing initially in the same density histogram bin. Hence the resulting value $\langle \tau(z) \rangle$ was attributed to the bins' centers $z = z_i \pm \delta z/2$.

C Mean first-passage time: proof of Eq. (3)

We first review exact results for the first-passage time statistics of one-dimensional diffusion processes. Let $P(x, t | x_0, 0)$ be the probability density for the process to be in a state $x(t) = x$ at a time t given that its initial state was $x(0) = x_0$. We assume that this probability density evolves according to a general Fokker-Planck equation

$$\frac{\partial P}{\partial t} = -\frac{\partial}{\partial x} [a(x)P] + \frac{1}{2} \frac{\partial^2}{\partial x^2} [b(x)P] \quad (10)$$

with two real-valued functions $a(x)$ and $b(x) > 0$. Exact formal expressions for several first-passage time statistics have been previously reported for this class of systems.^{64,87} We consider here escape of a molecule with the initial position $x(0) = z$ through one of the two boundaries of the passage corridor $[z - L, z + L]$ with $L > 0$. The probability $P_-(z)$ and $P_+(z)$ for the system to first reach the boundary at $z - L$ and $z + L$, respectively, are given by

$$P_-(z) = \frac{\int_{z-L}^{z+L} dy \pi(y)}{\int_{z-L}^{z+L} dy \pi(y)}, \quad P_+(z) = \frac{\int_{z-L}^z dy \pi(y)}{\int_{z-L}^{z+L} dy \pi(y)}, \quad (11)$$

with the auxiliary function $\pi(y)$ defined as

$$\pi(y) \equiv \exp\left(-\int^y dx \frac{2a(x)}{b(x)}\right). \quad (12)$$

The mean first-passage time for the system to first reach either the boundary at $z - L$ or the boundary at $z + L$ is then given by

$$\langle \tau(z) \rangle = \int_z^{z+L} dy \pi(y) I(y) - P_-(z) \int_{z-L}^{z+L} dy \pi(y) I(y), \quad (13)$$

in which the functions $P_-(z)$ and $\pi(y)$ are given by Eqs. (11) and (12), respectively, whereas

$$I(y) \equiv \int_{z-L}^y \frac{2dx}{b(x)\pi(x)}. \quad (14)$$

The diffusion model that we use to describe fluctuations of water density is governed by the Fokker-Planck equation [Eq.(1)],

copied here for convenience

$$\frac{\partial P(z, t)}{\partial t} = \frac{\partial}{\partial z} \left(\beta D(z) P(z, t) \frac{\partial U(z)}{\partial z} + D(z) \frac{\partial P(z, t)}{\partial z} \right),$$

which corresponds to Eq. (10) with

$$a(x) = -\beta D(x) U'(x) + D'(x), \quad b(x) = 2D(x). \quad (15)$$

Specializing Eqs. (12) and (14) to functions given by Eq. (15) we evaluate the auxiliary functions

$$\pi(y) = \frac{e^{\beta U(y)}}{D(y)}, \quad I(y) \equiv \int_{z-L}^y dx e^{-\beta U(x)}, \quad (16)$$

which resemble the inverse Boltzmann factor and the partition function, respectively. By substituting Eq. (16) into (11) and (13), we obtain the following explicit formulas for the passage probabilities

$$P_-(z) = \frac{\int_{z-L}^{z+L} dy e^{\beta U(y)}/D(y)}{\int_{z-L}^{z+L} dy e^{\beta U(y)}/D(y)}, \quad P_+(z) = \frac{\int_{z-L}^z dy e^{\beta U(y)}/D(y)}{\int_{z-L}^{z+L} dy e^{\beta U(y)}/D(y)}, \quad (17)$$

and the mean first-passage time

$$\begin{aligned} \langle \tau(z) \rangle &= \int_z^{z+L} \frac{dy}{D(y)} \int_{z-L}^y dx e^{-\beta[U(x)-U(y)]} \\ &- P_-(z) \int_{z-L}^{z+L} \frac{dy}{D(y)} \int_{z-L}^y dx e^{-\beta[U(x)-U(y)]}. \end{aligned} \quad (18)$$

Equations (17) and (18) are amenable to a complete analytical treatment only in special cases. For a sufficiently small L we may approximate the effective potential by a truncated power-series expansion

$$U(y) \simeq U(z) + (y - z)h + O(y^2), \quad (19)$$

which holds for $-L < y - z < L$ with $h \equiv U'(z)$. Because the diffusion coefficient is a strictly positive quantity, to preserve this property we use the approximation

$$D(y) \simeq D(z) e^{\kappa(y-z) + O(y^2)}, \quad (20)$$

in which $\kappa = D'(z)/D(z)$ is the logarithmic derivative of $D(z)$. The above equation implies a linear expansion of the logarithm of the diffusion coefficient $\ln D(y) \simeq \ln D(z) + \kappa(y - z) + O(y^2)$. For the approximate Eqs. (19) and (20) the formulas of the passage probabilities [Eq. (17)] read

$$P_-(z) \simeq \frac{1}{1 + e^{-L(\beta h - \kappa)}}, \quad P_+(z) \simeq \frac{1}{1 + e^{L(\beta h - \kappa)}}. \quad (21)$$

Eqs. (19)–(21) plugged into (18) lead to the following approximate expression for the mean first-passage time

$$\langle \tau(z) \rangle \simeq \frac{\cosh[(\beta h + \kappa)L/2] / \cosh[(\beta h - \kappa)L/2] - 1}{\kappa \beta h D(z)}. \quad (22)$$

The limit $\kappa \rightarrow 0$ of Eq. (22) yields Eq. (3), viz.

$$\langle \tau(z) \rangle \simeq \frac{L \tanh(L\beta k/2)}{D(z)\beta k}. \quad (23)$$

The limit $h \rightarrow 0$ of Eq. (3) gives in its turn the formula of the mean

first-passage time in bulk water

$$\langle \tau_{\text{bulk}} \rangle = \frac{L^2}{2D_{\text{bulk}}}, \quad (24)$$

in which we have identified $\langle \tau(z) \rangle \rightarrow \langle \tau_{\text{bulk}} \rangle$ and $D(z) \rightarrow D_{\text{bulk}}$.

D Linear-order effect of inhomogeneous diffusion

In this Appendix we show that the linear-order effect of inhomogeneous diffusion is negligible in our estimations of the coefficient $D(z)$ (Sec. 4). From Eq. (22) we can express the diffusion coefficient as

$$D(z) = \theta(h, \kappa) / \langle \tau(z) \rangle, \quad (25)$$

in which

$$\theta(h, \kappa) = \frac{\cosh[(\beta h + \kappa)L/2] / \cosh[(\beta h - \kappa)L/2] - 1}{\kappa \beta h}$$

depends only on the slope of the effective potential h and the unknown linear-order diffusion parameter κ .

The effective potential of water molecules and the mean first-passage times $\langle \tau(z) \rangle$ have been extracted from our molecular-dynamics simulations (Sec. 4). Therefore we need to find only the parameter κ in order to evaluate Eq. (25) and, in particular, the coefficient $\theta(h, \kappa)$ to the linear-order in z . The parameter κ can be inferred from the first-passage probabilities that we reported in Sec. 5 (right panels in Fig. (8)) by using Eq. (21):

$$\kappa = \beta h + \log[P_+(z)/P_-(z)]/L.$$

As shown in Fig. 10, Equation (25) that incorporates the linear-order correction due to the variation of $D(z)$ gives estimates almost identical to those of Sec. 5. This fact confirms that the mobility of water molecules changes much slower than their effective potential.

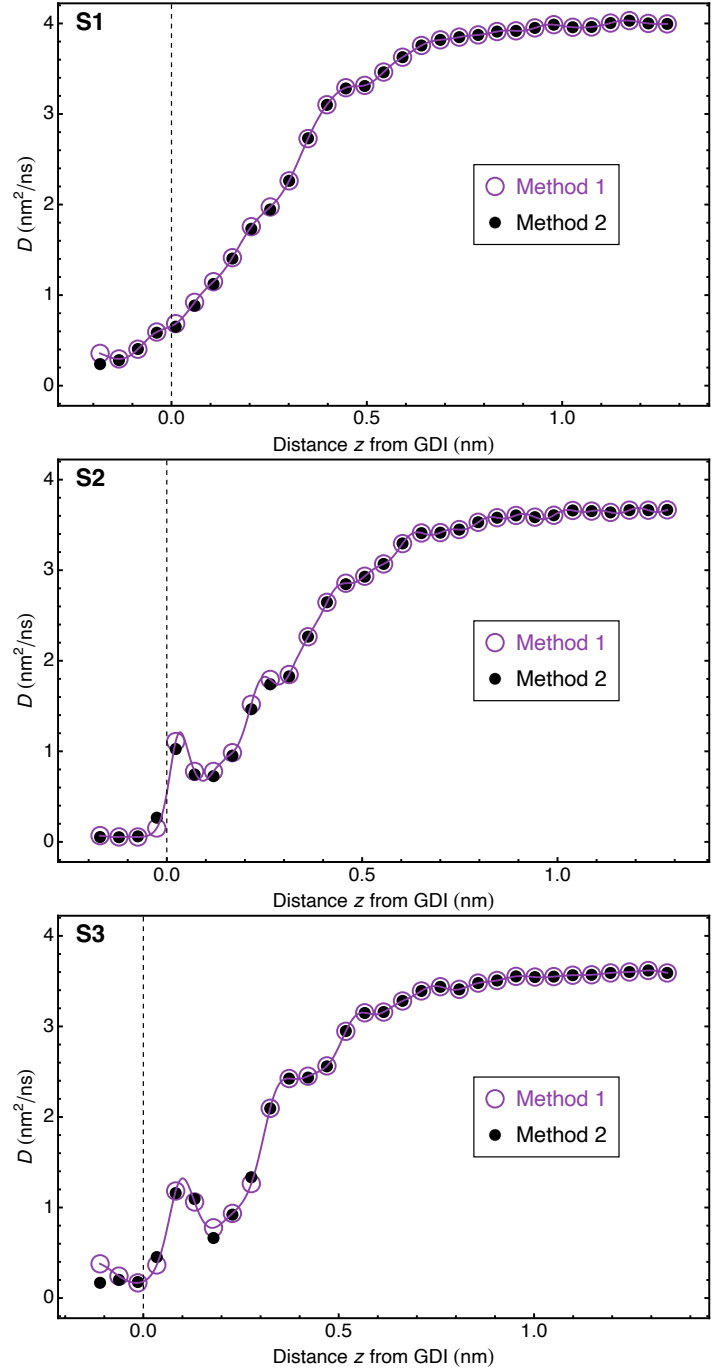


Fig. 10 Comparison of the diffusion coefficient values estimated by the method of Sec. 5 (Method 1) and the method of Appendix D (Method 2) that takes into account the linear-order variation of $D(z)$ as a function of the distance to the Gibbs dividing interface with one of the three glutamine surfaces.

Notes and references

- 1 P. W. Fenimore, H. Frauenfelder, B. H. McMahon and F. G. Parak, *Proceedings of the National Academy of Sciences of the United States of America*, 2002, **99**, 16047–16051.
- 2 S. Yang, J. N. Onuchic, A. E. García and H. Levine, *Journal of Molecular Biology*, 2007, **372**, 756–763.
- 3 V. J. Van Hijkoop, A. J. Dammers, K. Malek and M. O. Coppens, *Journal of Chemical Physics*, 2007, **127**, year.
- 4 R. B. Best and G. Hummer, *Proceedings of the National Academy of Sciences of the United States of America*, 2010, **107**, 1088–1093.
- 5 R. B. Best, G. Hummer and W. A. Eaton, *Proceedings of the National Academy of Sciences of the United States of America*, 2013, **110**, 17874–17879.
- 6 M. Hinczewski, Y. Von Hansen, J. Dzubiella and R. R. Netz, *Journal of Chemical Physics*, 2010, **132**, year.
- 7 Y. von Hansen, I. Kalcher and J. Dzubiella, *The Journal of Physical Chemistry B*, 2010, **114**, 13815–13822.
- 8 J. Wong-ekkabut and M. Karttunen, *Journal of Biological Physics*, 2016, **42**, 133–146.
- 9 S. Sharma and P. Biswas, *Journal of Physics Condensed Matter*, 2018, **30**, year.
- 10 E. W. Knapp and I. Muegge, *The Journal of Physical Chemistry*, 1993, **97**, 11339–11343.
- 11 I. Muegge and E. W. Knapp, *Physical Chemistry The Journal*, 1995, **0**, year.
- 12 F. Sedlmeier, Y. von Hansen, L. Mengyu, D. Horinek and R. R. Netz, *Journal of Statistical Physics*, 2011, **145**, 240–252.
- 13 K. Amann-Winkel, M.-C. Bellissent-Funel, L. E. Bove, T. Lortering, A. Nilsson, A. Paciaroni, D. Schlesinger and L. Skinner, *Chemical reviews*, 2016, **116**, 7570–7589.
- 14 R. H. Pearson and I. Pascher, *Nature*, 1979, **281**, 499.
- 15 J. S. Finer-Moore, A. A. Kossiakoff, J. H. Hurley, T. Earnest and R. M. Stroud, *Proteins: Structure, Function, and Bioinformatics*, 1992, **12**, 203–222.
- 16 D. Svergun, S. Richard, M. Koch, Z. Sayers, S. Kuprin and G. Zaccai, *Proceedings of the National Academy of Sciences*, 1998, **95**, 2267–2272.
- 17 F. Merzel and J. C. Smith, *Proceedings of the National Academy of Sciences*, 2002, **99**, 5378–5383.
- 18 G. Otting, E. Liepinsh and K. Wuthrich, *Science*, 1991, **254**, 974–980.
- 19 E. Liepinsh, G. Otting and K. Wüthrich, *Nucleic acids research*, 1992, **20**, 6549–6553.
- 20 N. V. Nucci, M. S. Pometun and A. J. Wand, *Journal of the American Chemical Society*, 2011, **133**, 12326–12329.
- 21 N. V. Nucci, M. S. Pometun and A. J. Wand, *Nature structural & molecular biology*, 2011, **18**, 245.
- 22 Z. Brotzakis, C. Groot, W. H. Brandeburgo, H. Bakker and P. Bolhuis, *The Journal of Physical Chemistry B*, 2016, **120**, 4756–4766.
- 23 D. Russo, G. Hura and T. Head-Gordon, *Biophysical journal*, 2004, **86**, 1852–1862.
- 24 K. Wood, M. Plazanet, F. Gabel, B. Kessler, D. Oesterheld, D. Tobias, G. Zaccai and M. Weik, *Proceedings of the National Academy of Sciences*, 2007, **104**, 18049–18054.
- 25 G. Schirò, Y. Fichou, F.-X. Gallat, K. Wood, F. Gabel, M. Moulin, M. Härtlein, M. Heyden, J.-P. Colletier, A. Orecchini *et al.*, *Nature communications*, 2015, **6**, 6490.
- 26 D. Russo, R. K. Murarka, J. R. Copley and T. Head-Gordon, *The Journal of Physical Chemistry B*, 2005, **109**, 12966–12975.
- 27 A. R. Bizzarri and S. Cannistraro, *Molecular dynamics of water at the protein- solvent interface*, 2002.
- 28 F. Pizzitutti, M. Marchi, F. Sterpone and P. J. Rossky, *The Journal of Physical Chemistry B*, 2007, **111**, 7584–7590.
- 29 V. A. Makarov, B. K. Andrews, P. E. Smith and B. M. Pettitt, *Biophysical journal*, 2000, **79**, 2966–2974.
- 30 M. Marchi, F. Sterpone and M. Ceccarelli, *Journal of the American Chemical Society*, 2002, **124**, 6787–6791.
- 31 R. H. Henchman and J. A. McCammon, *Protein Science*, 2002, **11**, 2080–2090.
- 32 T. Li, A. A. Hassanali, Y.-T. Kao, D. Zhong and S. J. Singer, *Journal of the American Chemical Society*, 2007, **129**, 3376–3382.
- 33 A. C. Fogarty and D. Laage, *The Journal of Physical Chemistry B*, 2014, **118**, 7715–7729.
- 34 A. Luise, M. Falconi and A. Desideri, *Proteins: Structure, Function, and Bioinformatics*, 2000, **39**, 56–67.
- 35 P. J. Rossky and M. Karplus, *Journal of the American Chemical Society*, 1979, **101**, 1913–1937.
- 36 M. Heyden and D. J. Tobias, *Physical review letters*, 2013, **111**, 218101.
- 37 A. E. García and G. Hummer, *Proteins: Structure, Function, and Bioinformatics*, 2000, **38**, 261–272.
- 38 D. Laage, G. Stirnemann and J. T. Hynes, *The Journal of Physical Chemistry B*, 2009, **113**, 2428–2435.
- 39 M.-C. Bellissent-Funel, A. Hassanali, M. Havenith, R. Henchman, P. Pohl, F. Sterpone, D. van der Spoel, Y. Xu and A. E. Garcia, *Chemical Reviews*, 2016, **116**, 7673–7697.
- 40 P. Rani and P. Biswas, *The Journal of Physical Chemistry B*, 2015, **119**, 13262–13270.
- 41 S. Pronk, E. Lindahl and P. M. Kasson, *Nature communications*, 2014, **5**, 3034.
- 42 S. Dellerue and M.-C. Bellissent-Funel, *Chemical Physics*, 2000, **258**, 315–325.
- 43 D. Laage and J. T. Hynes, *Proceedings of the National Academy of Sciences of the United States of America*, 2007, **104**, 11167–11172.
- 44 D. Laage, T. Elsaesser and J. T. Hynes, *Chemical Reviews*, 2017, **117**, 10694–10725.
- 45 P. Ball, *Chemical Reviews*, 2008, **108**, 74–108.
- 46 Y. Levy and J. N. Onuchic, *Annual Review of Biophysics and Biomolecular Structure*, 2006, **35**, 389–415.
- 47 *Proceedings of the National Academy of Sciences of the United States of America*, 2002, **99**, 11884–11889.

- 48 R. Nelson, M. R. Sawaya, M. Balbirnie, A. Ø. Madsen, C. Riek, R. Grothe and D. Eisenberg, *Nature*, 2005, **435**, 773–778.
- 49 A. W. P. Fitzpatrick, G. T. Debelouchina, M. J. Bayro, D. K. Clare, M. A. Caporini, V. S. Bajaj, C. P. Jaroniec, L. Wang, V. Ladizhansky, S. A. Müller, C. E. MacPhee, C. A. Waudby, H. R. Mott, A. De Simone, T. P. J. Knowles, H. R. Saibil, M. Vendruscolo, E. V. Orlova, R. G. Griffin and C. M. Dobson, *Proceedings of the National Academy of Sciences*, 2013, **110**, 5468–5473.
- 50 M. A. Wälti, F. Ravotti, H. Arai, C. G. Glabe, J. S. Wall, A. Böckmann, P. Güntert, B. H. Meier and R. Riek, *Proceedings of the National Academy of Sciences*, 2016, **113**, E4976–E4984.
- 51 U. Shimanovich, D. Pinotsi, K. Shimanovich, N. Yu, S. Bolisetti, J. Adamcik, R. Mezzenga, J. Charmet, F. Vollrath, E. Gazit, C. M. Dobson, G. K. Schierle, C. Holland, C. F. Kaminski and T. P. J. Knowles, *Macromolecular Bioscience*, 2018, **18**, 1700295.
- 52 D. Pinotsi, L. Grisanti, P. Mahou, R. Gebauer, C. F. Kaminski, A. Hassanali and G. S. Kaminski Schierle, *Journal of the American Chemical Society*, 2016, **138**, 3046–3057.
- 53 K. H. Jong, Y. T. Azar, L. Grisanti, A. D. Stephens, S. T. E. Jones, D. Credgington, G. S. Kaminski Schierle and A. Hassanali, *Phys. Chem. Chem. Phys.*, 2019, **21**, 23931–23942.
- 54 A. D. Stephens, M. N. Qaisrani, M. T. Ruggiero, S. T. Jones, E. Poli, A. D. Bond, P. J. Woodhams, E. M. Kleist, L. Grisanti, R. Gebauer, J. A. Zeitler, D. Credgington, A. Hassanali and G. S. Kaminski Schierle, *bioRxiv*, 2020.
- 55 L. Grisanti, D. Pinotsi, R. Gebauer, G. S. Kaminski Schierle and A. A. Hassanali, *Phys. Chem. Chem. Phys.*, 2017, **19**, 4030–4040.
- 56 T. Wang, H. Jo, W. F. DeGrado and M. Hong, *Journal of the American Chemical Society*, 2017, **139**, 6242–6252.
- 57 P. Liu, E. Harder and B. J. Berne, *Journal of Physical Chemistry B*, 2004, **108**, 6595–6602.
- 58 G. Hummer, *New Journal of Physics*, 2005, **7**, year.
- 59 W. Olivares-Rivas, P. J. Colmenares and F. López, *The Journal of Chemical Physics*, 2013, **139**, 074103.
- 60 M. N. Qaisrani, L. Grisanti, R. Gebauer and A. Hassanali, *Physical Chemistry Chemical Physics*, 2019, **21**, 16083–16094.
- 61 S. Redner, *A guide to first-passage processes*, Cambridge University Press, 2001.
- 62 R. Metzler, G. Oshanin and S. Redner, *First-passage phenomena and their applications*, World Scientific, 2014.
- 63 J. Masoliver, B. J. West and K. Lindenberg, *Physical Review A*, 1987, **35**, 3086.
- 64 P. Hänggi, P. Talkner and M. Borkovec, *Reviews of modern physics*, 1990, **62**, 251.
- 65 I. Sokolov, *Physical review letters*, 2003, **90**, 080601.
- 66 S. Condamin, O. Bénichou, V. Tejedor, R. Voituriez and J. Klafter, *Nature*, 2007, **450**, 77–80.
- 67 T. Koren, M. A. Lomholt, A. V. Chechkin, J. Klafter and R. Metzler, *Physical review letters*, 2007, **99**, 160602.
- 68 T. G. Mattos, C. Mejía-Monasterio, R. Metzler and G. Oshanin, *Physical Review E*, 2012, **86**, 031143.
- 69 A. J. Bray, S. N. Majumdar and G. Schehr, *Advances in Physics*, 2013, **62**, 225–361.
- 70 A. Pal and S. Reuveni, *Physical review letters*, 2017, **118**, 030603.
- 71 D. Hartich and A. Godec, *Journal of Statistical Mechanics: Theory and Experiment*, 2019, **2019**, 024002.
- 72 A. Szabo, K. Schulten and Z. Schulten, *The Journal of chemical physics*, 1980, **72**, 4350–4357.
- 73 E. A. Galburt, S. W. Grill, A. Wiedmann, L. Lubkowska, J. Choy, E. Nogales, M. Kashlev and C. Bustamante, *Nature*, 2007, **446**, 820–823.
- 74 É. Roldán, A. Lisica, D. Sánchez-Taltavull and S. W. Grill, *Physical Review E*, 2016, **93**, 062411.
- 75 X. Yang, C. Liu, Y. Li, F. Marchesoni, P. Hänggi and H. Zhang, *Proceedings of the National Academy of Sciences*, 2017, **114**, 9564–9569.
- 76 J. Gladrow, M. Ribezzi-Crivellari, F. Ritort and U. F. Keyser, *Nature communications*, 2019, **10**, 1–9.
- 77 S. Chandrasekhar, *The Astrophysical Journal*, 1943, **97**, 263.
- 78 S. N. Majumdar, *Curr. Sci.*, 2005, **88**, 2076–2092.
- 79 G. Wergen, M. Bogner and J. Krug, *Physical Review E*, 2011, **83**, 051109.
- 80 S. Singh, P. Menczel, D. S. Golubev, I. M. Khaymovich, J. T. Peltonen, C. Flindt, K. Saito, É. Roldán and J. P. Pekola, *Physical review letters*, 2019, **122**, 230602.
- 81 A. Berezhkovskii and G. Hummer, *Physical review letters*, 2002, **89**, 064503.
- 82 V. J. van Hijkoop, A. J. Dammers, K. Malek and M.-O. Coppens, *The Journal of chemical physics*, 2007, **127**, 08B613.
- 83 F. Sedlmeier, Y. von Hansen, L. Mengyu, D. Horinek and R. R. Netz, *Journal of Statistical Physics*, 2011, **145**, 240–252.
- 84 C. Calero, J. Faraudo and M. Aguilera-Arzo, *Physical Review E*, 2011, **83**, 021908.
- 85 S. Sharma and P. Biswas, *Journal of Physics: Condensed Matter*, 2017, **30**, 035101.
- 86 M. J. Abraham, T. Murtola, R. Schulz, S. Páll, J. C. Smith, B. Hess and E. Lindahl, *SoftwareX*, 2015, **1**, 19–25.
- 87 N. S. Goel and N. Richter-Dyn, *Stochastic Models in Biology*, Elsevier, 2016.
- 88 A. W. Lau and T. C. Lubensky, *Physical Review E - Statistical, Nonlinear, and Soft Matter Physics*, 2007, **76**, year.
- 89 É. Roldán, I. Neri, M. Dörpinghaus, H. Meyr and F. Jülicher, *Physical Review Letters*, 2015, **115**, year.
- 90 I. Neri, É. Roldán and F. Jülicher, *Physical Review X*, 2017, **7**, 011019.
- 91 P. Krapivsky and S. Redner, *Journal of Statistical Mechanics: Theory and Experiment*, 2018, **2018**, 093208.
- 92 R. Metzler, E. Barkai and J. Klafter, *Deriving fractional Fokker-Planck equations from a generalised master equation*, 4, 1999.

- 93 E. Barkai, R. Metzler and J. Klafter, *From continuous time random walks to the fractional Fokker-Planck equation*.
- 94 S. Y. Sheu and D. Y. Yang, *Journal of Physical Chemistry B*, 2010, **114**, 16558–16566.
- 95 S. A. Loos, S. M. Hermann and S. H. Klapp, *arXiv preprint arXiv:1910.08372*, 2019.
- 96 O. Bj rnehlm, M. H. Hansen, A. Hodgson, L.-M. Liu, D. T. Limmer, A. Michaelides, P. Pedevilla, J. Rossmeis, H. Shen, G. Tocci, E. Tyrode, M.-M. Walz, J. Werner and H. Bluhm, *Chemical Reviews*, 2016, **116**, 7698–7726.
- 97 F. Giberti and A. A. Hassanali, *The Journal of Chemical Physics*, 2017, **146**, 244703.
- 98 E. Poli, K. H. Jong and A. Hassanali, *Nature Communications*, 2020, **11**, 901.
- 99 G. Ramakrishnan, M. Gonz lez-Jim nez, A. J. Laphorn and K. Wynne, *The Journal of Physical Chemistry Letters*, 2017, **8**, 2964–2970.
- 100 M. Tros, L. Zheng, J. Hunger, M. Bonn, D. Bonn, G. J. Smits and S. Woutersen, *Nature Communications*, 2017, **8**, 904.
- 101 W. L. Jorgensen, D. S. Maxwell and J. Tirado-Rives, *Journal of the American Chemical Society*, 1996, **118**, 11225–11236.
- 102 W. L. Jorgensen, J. Chandrasekhar, J. D. Madura, R. W. Impey and M. L. Klein, *The Journal of chemical physics*, 1983, **79**, 926–935.
- 103 W. L. Jorgensen and J. D. Madura, *Molecular Physics*, 1985, **56**, 1381–1392.
- 104 T. Darden, D. York and L. Pedersen, *The Journal of chemical physics*, 1993, **98**, 10089–10092.
- 105 B. Hess, H. Bekker, H. J. Berendsen and J. G. Fraaije, *Journal of computational chemistry*, 1997, **18**, 1463–1472.
- 106 G. Bussi, D. Donadio and M. Parrinello, *The Journal of chemical physics*, 2007, **126**, 014101.
- 107 L. N. Trefethen, *Spectral Methods in MATLAB*, SIAM, 2000.